VOLUME 7 NO. 2
DEC 2010
ISSN 1675-7009

SCIENTIFIC RESEARCH JOURNAL

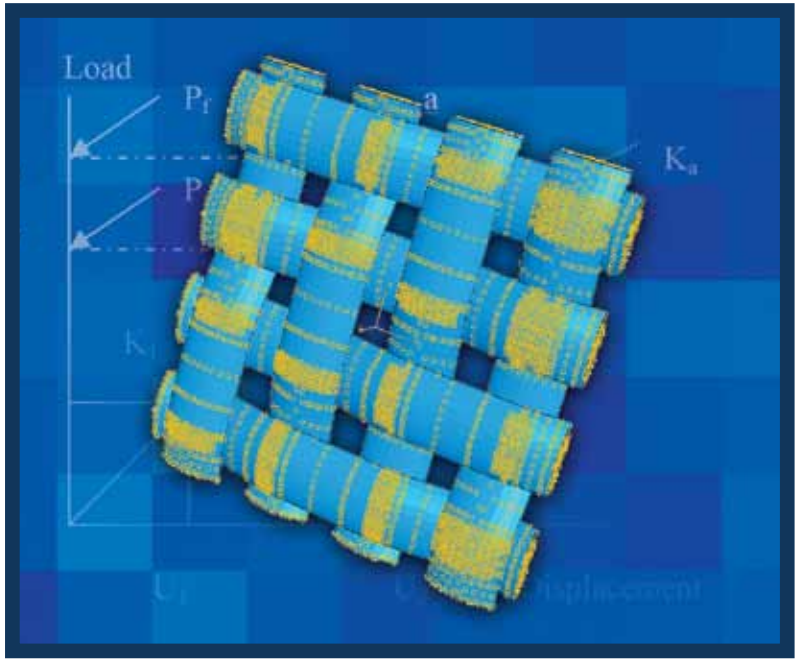

RESEARCH MANAGEMENT INSTITUTE

SCIENTIFIC RESEARCH JOURNAL

Scientific Research Journal is jointly published by Research Management Institute (RMI) and University Publication Centre (UPENA), Universiti Teknologi MARA, 40450 Shah Alam, Selangor, Malaysia.

SCIENTIFIC RESEARCH JOURNAL

Vol. 7 No. 2 **December 2010** **ISSN 1675-7009**

Hyperelastic and Elastic-Plastic Approaches for Modelling Uniaxial Tensile Performance of Woven Fabrics

Yahya, M.F.[1,2] and Chen, X.[1]

[1]School of Materials, University of Manchester, M60 1QD, Manchester, United Kingdom
[2]Faculty of Applied Sciences, Universiti Teknologi MARA 40450 Shah Alam, Selangor, Malaysia
[2]Email: faizulmy@gmail.com

ABSTRACT

This article presents the findings of experimental and finite element simulation warp direction uniaxial tensile testing of plain 1/1, 2/2 twill and 8 ends satin woven fabrics with respect to a woven fabric model developed in IGES using UniverFilter. Woven fabrics have been specifically configured as a balanced weave thereby allowing systematic investigation of the effect of uniaxial tensile stress on the weave. Static automatic incrementation of large representative volume elements has enabled characterisation of the response of two-dimensional woven fabrics under uniaxial tensile stress with respect to hyperelastic and elastic-plastic material properties. Plain 1/1 and 8 ends satin woven fabrics were well-described by the hyperelastic model and the elastic-plastic model predicted extended strain percentages. The modelling indicates that satin woven fabric possesses the lowest strain distribution and compression stress in the unloaded weft direction compared to plain and twill woven fabrics.

Keywords: *Finite element analysis, CAD, uniaxial tensile, stress-strain*

ISSN 1675-7009

Introduction

The rapid growth of technical textiles has contributed to the development of high performance textile materials used in various applications and conditions. Technical textile areas, including automotive, medical, geotextiles, composites, sports and leisure, and protective clothing, have recorded significant growth in terms of market demand [1]. Textile materials have been developed to the extent where they have high resilience, toughness and impact resistance, prime examples include Nylon 6 and Nylon 6,6, which are used in load bearing applications such as aircraft and car tires, parachutes and conveyor belts. Polyester, which has good dimensional stability and high dynamic energy absorption, has been successfully used in the construction of artificial ligaments and arteries, car seats and sailcloth fabric [2]. The mechanical and physical properties of woven fabrics are influenced by the fibre, yarn and fabric configurations. For example, the use of higher ends per cm result in heavier woven fabrics with better tensile strength. Tensile strength is regarded as a fundamental test, since it provides insight regarding material resistance to failure and is closely related to other failure modes, such as compression, bending and impact. A systematic approach has been adopted in order to normalise the fibre and yarn properties so that the weave influence upon uniaxial tension behaviour can be investigated and evaluated. The experimental performance of two-dimensional plain 1/1, twill 2/2 and 8 ends satin woven fabrics, designed with comparable fibre groups and yarn linear densities, are evaluated with respect to simulations. The simulations were performed using three-dimensional models of the woven fabrics and analyzed using finite element analysis. The research has been performed in order to review the roles of woven fabric structures roles in textile composites applications particularly for transportation, defence, civil engineering, aerospace and sports.

Tensile Behaviour of Woven Fabrics

The tensile behaviour of woven fabrics has been the subject of interest for many researchers [3]. In general, the tensile behaviour of woven fabrics can be analyzed both experimentally and analytically with respect to theoretical modelling. Experiments is the best way to obtain direct information regarding the mechanical properties of woven fabrics,

however it is also generates sample waste. Literature on tensile deformation mechanics is extensive, but primarily focuses upon the evaluation of the tensile behaviour upon exposure to biaxial forces. For example, Hearle and Shanahan [4] proposed an energy model to investigate the biaxial performance of woven fabric, whereby they showed that the total energy, U, in a fabric system comprises of forces acting in the warp, F_x, and weft, F_y, directions, where in general the warp extension, x, and weft extension, y, can be achieved by minimizing the energy with respect to Equation 1:

$$U = -F_x x - F_y y \tag{1}$$

An analytical approach is suitable for evaluating simple two-dimensional geometric models; however there is inherent greater mathematical complexity in the design and solution if larger woven structures are to be analyzed. Therefore, approximate solutions are adopted for predicting the mechanical behaviour of large representative elements in woven fabrics and finite element analysis is one of the most accepted techniques used in solution approximation of solutions. Finite element analysis is used to solve large structural problems by discretising the problem into smaller sections or elements connected by a series of nodal points. Static analysis of the element stiffness in a matrix [5] is calculated with respect to Equation 2:

$$[K](u) = F \tag{2}$$

In the equation, K is the element stiffness matrix, u is a displacement vector and F is a force vector. The following example illustrates how a force vector is established with respect to the node displacements, u, between node 1 and 2 [5].

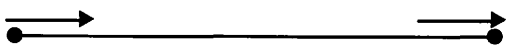

Node 1 , U_1 Node 2, U_2

at Node 2, $F_2 = K(u_2 - u_1)$ (3)

at Node 1, $F_1 = -K(u_2 - u_1)$ (4)

These functions can be re-written in matrix form as:

$$\begin{bmatrix} K & -K \\ -K & K \end{bmatrix} \begin{Bmatrix} u_1 \\ u_2 \end{Bmatrix} = \begin{Bmatrix} F_1 \\ F_2 \end{Bmatrix} \quad (5)$$

Finite element analysis has been well used to measure woven fabric mechanical properties, in particularly the tensile strength. Tarfaoui *et al.* [6, 7] stated that finite element analysis can be used to represent fabric geometrical properties and their symmetries with minimal assumptions; in the case of weave mesh structures very close representations are possible. Tresca stress analysis was performed on a three dimensional model of a plain woven fabric undergoing biaxial's stress using a 4-node quadrangle element. Provatidis [8] stated that the non-linear behaviour of plain woven fabrics during biaxial tensile testing will increase with the modulus of elasticity when plain weave hexahedron elements with Hertzian-surface to surface contacts are adopted. In composites, Glaessgen *et al.* [9] published significant findings, which provided validation of experimental findings with respect to finite element simulation and analysis of both dry and laminated plain woven glass. A three dimensional model of a plain woven fabric was established by connecting lines using Bezier algorithms for yarn faces, which later form a volume for the purposes of finite element analysis. The yarn cross section was designed in a circular form with quadratic tetrahedral elements in order to facilitate data generation during descretisation. While cited researchers have developed the application of finite element analysis for modelling woven fabrics through the assumption of a circular cross section; the yarn cross section should in actual fact be presented as non-circular, because in most applications yarns in woven fabrics are compressed and flattened due to the forces imposed upon them. Other researchers have adopted a lenticular yarn shape for finite element analysis. Gasser[10] evaluated the biaxial stress performance of plain glass, 3 × 1glass twill, 2 × 2carbon twill and 2.5D carbon fabrics with respect to experimental and numerical analysis by assuming yarn behaviour to be orthotropic under shear (G_{12}, G_{13}, G_{13}) with Poisson ratios (V_{12}, V_{13}, V_{23}) zero in all directions and a lower transverse modulus, E_2, than longitudinal modulus, E_1. It was reported in the work that the plain weave exhibits higher nonlinearity and the lowest loading compared to twill 2/2 and twill 3/1. Boisse *et al.* [11] succesfully solved the numerical convergence problem

associated with small transverse elastic orthotropic moduli for biaxial and shear deformation of an hourglass-shaped unbalanced glass plain woven fabric. Duan [12] employed a lenticular yarn cross section in order to evaluate the ballistic performance of aramid plain woven fabric. By simulating a 600 tex glass balanced plain woven fabric using representative volume elements (RVE) Thammandra [13] determined that the knee phenomenon can be reduced by applying a biaxial force during the composite forming process. In the context of this research the biaxial response of plain woven fabrics was performed using ABAQUS using lenticular shaped yarn with transverse isotropic behaviour.

The consistent stream of publications regarding modelling of the mechanical behaviour of woven fabrics, particularly the tensile strength, is indicative of significant research interest in this field, whereby the simulation of complex woven fabric structures is becoming increasingly more realistic and elucidating combined with improved simulation efficiency and decreasing computational time. As in the earlier discussion of Hearle's works, numerous other researchers have focussed upon the modelling of the biaxial response of woven fabrics. Boisse's simulations [14] indicate that if equivalent forces build in both the warp and weft directions this corresponds to stronger fabrics and reduces the knee effect found in composites, which is in agreement with Thammandra's [13] work. The research presented herein considers the effect of uniaxial forces on the three main woven structures; namely, plain, twill and satin. Modelling work will initially be used to validate respective experimental and simulation tensile strength results, but will be used later to investigate the compressional effect generated between the warp and weft yarns due to uniaxial tensile loading. Uniaxial tensile analysis is performed on square two-dimensional woven manufactured fabrics and their geometrical model equivalents. The three dimensional geometrical woven fabric models were developed using an in-house CAD program, UniverFilter, and modelled using the finite element analysis package ABAQUS. The yarns in the finite element models are considered to be hyperelastic and elastic-plastic. Simulating uniaxial hyperelastic yarn testing enabled determination of the strain energy stored in the material unit volume at each material point. This material behaviour was exploited since it enables analysis of large strain deformations and non-linear geometrical structures. The model assumes that materials behave isotropically when stretched and that yarn behaviour changes from elastic to plastic upon exceeding the yield point [15]. Yarn surface element contacts in the woven fabrics are defined to be fixed throughout the analysis as suggested by Leaf [16, 17] and the

warp and weft yarns are meshed automatically yielding an irregular mesh configuration thereby ensuring stable numerical solution convergence at each incremental step. The following section discusses the specifics of the simulation work in greater detail.

Research Tasks

Yarn Tensile Test

Fibre and yarn properties must be defined before the woven fabric models can be produced. The properties of the woven fabric models may be is represented with respect to the density in g cm^{-2} and the Poisson ratio. The fibre density, 1.44 g cm^{-2}, used in this research was adopted from existing literature [18], whereas the aramid fibre Poisson ratio and yarn elastic modulus were validated with respect to experimental yarn uniaxial tensile strength testing and the corresponding finite element analysis. Yarn tensile was performed using an Instron tensile tester machine according to the single yarn strength method, BS EN ISO 2062:1995.

The specimen length required to perform the tensile strength tests was 250 mm to which a load of 5000 N was applied. In general, there is a 0.5% deviation between the experimental and simulated yarn stress-strain results. Beyond 0.5% strain, kevlar yarn is reported to observe a linear trend until it exceeds the elastic point at 475 MPa of stress and

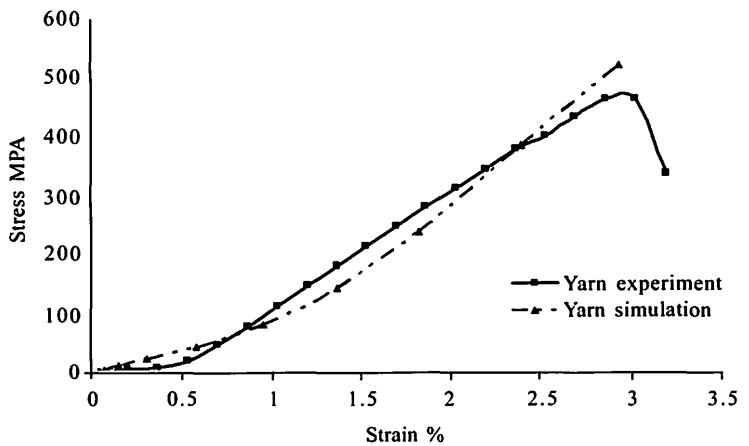

Figure 1: Yarn Experimental and Model Validation

3.03% of strain. The finite element analysis of the yarn assumes the material to be isotropically elastic, of a lenticular cross sectional shape, and possess a density of 1.44 g cm^{-3} and an elastic modulus of 19,000 MPa. The Poisson ratio was determined with respect to experimental and finite element analysis conversion at a value of 0.37; this value was used in the woven fabric models. The results of the finite element modelling are presented with respect to experimental findings in Figure 1 and indicate good correlation (1-2.25% deviation) between the simulated and experimental stress and strain results.

Woven Fabric Manufacture

Woven fabric manufacture is considered a significant stage since it provides the bases for the experimental, finite element and comparison anlaysis of the two, therefore consistency within the fabrication process is vital. Fabric weaving is a multi-step process requiring warping, draw-in, reed-in and weaving. The complete woven fabric specifications are presented in Table 1.

Table 1: Woven Fabric Specifications

Weave structures	Plain 1/1	Twill 2/2	8 Ends Satin
Fibre type	Kevlar 149	Kevlar 149	Kevlar 149
Poisson ratio	0.37	0.37	0.37
Yarn modulus (MPa)	19000	19000	19000
Warp Tex	157.5	157.5	157.5
Weft Tex	157.5	157.5	157.5
End / cm	8	8	8
Picks / cm	8	8	8
Warp crimp (%)	3.5	1.46	0.93
Weft crimp (%)	2.6	1.2	0.9
Fabric thickness (mm)	1.5	1.1	1.1
Fabric weight (g m^{-2})	259.7	255.4	254.32

To provide less friction between yarns and facilitate clear shedding, the warp beams were separated into four strands during warping, where each beam hosts 48 ends, with a maximum fabric width of 24 cm and a total of 192 woven fabric ends. Warp yarns were threaded onto the loom using a straight draw-in plan, whereupon draw-in and reed-in were commenced once all the beams had been assembled on the loom. The

Saurer dobby loom has 8 frames; warp yarns from the first beam were threaded through heald-eyes on healdframes number one and five. Similarly, warp yarns from the second beam were threaded through second and sixth healdframes respectively. Two warp yarns were subsequently threaded through one reed dent before weaving commenced.

Woven Fabric Tensile Strength Testing

The tensile strength of plain, twill 2/2 and 8-ends satin was determined using an Instron tensile tester machine using the force and elongation strip method, BS EN ISO 13934-1: 1999, on specimens of dimension 35 mm × 150 mm. The maximum load applied to the specimens was 5000 N, with cross head speed of 100 mm m^{-1}. The average tensile strength results in each direction were taken for five samples. Figures 2 and 3 present the woven fabric specimen dimensions prior to tensile strength testing and the stress and strain behaviour of plain, twill 2/2 and 8-ends satin weaves in the warp direction, respectively. In general, it is evident that the 8-ends satin weave exhibits the highest stress-strain, especially in the strain range 0.5-2%, compared to plain and twill 2/2 weaves and the least extension of only 1.2% at 15MPa, which may be attributed to the fact that loaded yarns are packed during uniaxial loading as a consequence of less crimp, which eventually contributes to high tensile stress-strain performance. Plain woven fabrics exhibit the lowest stress-strain results with a maximum of 24 MPa. Twill 2/2 and plain fabric weaves exhibit a 1.5% and 2.1% extension, respectively.

The higher crimp level present in plain woven fabrics may be responsible for the reduced stress experienced with respect to the increasing strain percentage. In general, tensile deformation occurs as soon as a load is applied to the woven fabrics and during lower strain percentages the woven fabric exhibits nonlinear behaviour and a low modulus of elasticity. Plain woven exhibits greater nonlinearity due to a volume of crimps compared to twill 2/2 and 8-ends satin. Once woven fabrics are fully extended thereby removing all crimps, the yarns will respond to the applied load. Consequently, higher moduli of elasticity will be recorded, since more stress is being generated even with very small strain increments.

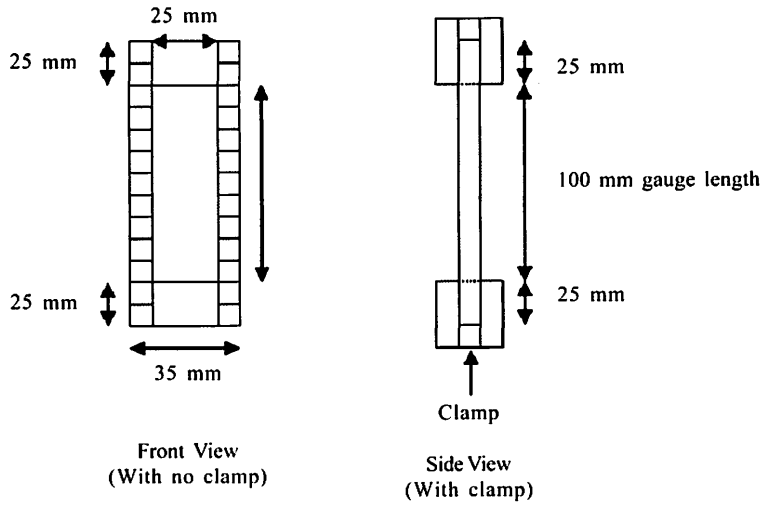

Figure 2: Tensile Specimen Dimensions

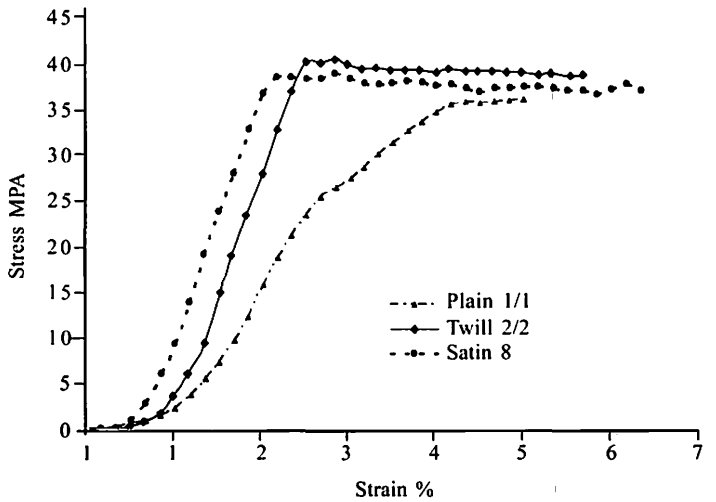

Figure 3: Tensile Results in the Warp Direction

Woven Fabric Geometrical Model Development

Woven fabrics must be properly represented or modelled for finite element analysis work. It is possible to adopt a global approach, in which the woven fabric is treated as a 2D or 3D plate. Both models can

be computationally solved efficiently, but there is no yarn to yarn interface as this approach neglects this microscopic factor [19]. Another approach uses a discontinuum, whereby warp and weft yarns are modelled and material definitions are made independently using a systematically determined adequate number of contacts points. In the work, plain 1/1, twill 2/2 and 8 ends satin were modelled by adopting the three dimensional discontinuum approach. For accurate modelling work, experimentally determined were applied to the respective woven fabric models, Table 1. Woven fabric models were established using the in-house weave CAD program, UniverFilter, which enabled rapid woven fabric model prototyping. Geometric model specifications, such as yarn modular lengths, yarn spacing, diameters, warp and weft weave angles and crimp formations, were based on the Pierce geometric model [20]. Microscope images were captured and analyzed to determine not only the cross sectional shapes, but also the areas and aspect ratios. Image analysis of fabric samples under 5× magnification enabled estimation of the yarn cross sectional shape, which is lenticular. Careful dimensional measurement of the microscopic images is vital since relaxed yarns normally take up larger cross sectional areas than firmly interlaced woven fabric yarns. Hence the yarn aspect ratio, *i.e.* the yarn width to thickness ratio, was determined using the smallest possible length. Figure 4 illustrates the yarn cross sectional shapes and areas determined during microscopic analysis. After careful consideration, the yarn width and thickness were taken to be 2.41 mm and 0.35 mm, respectively. If the yarn width is defined to be A and the thickness, B, then the yarn cross sectional lenticular area is 0.56 mm^2, with respect to Equations 6-9 [21].

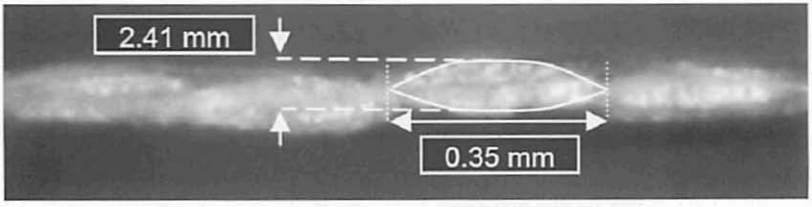

Figure 4: Yarn Cross Sectional Shape under Microscope

Yarn cross sectional area, $A = 2R^2 (\theta - \cos\theta \sin\theta)$ (6)

Aspect ratio, F; $$F = \frac{A}{B}$$ (7)

Arch angle, θ; $$\sin\theta = \frac{2F}{1+F^2} \quad (8)$$

Lenticular radius, R; $$R = \left(\frac{A^2 + B^2}{4B} \right) \quad (9)$$

Woven Model Generation

In order to create woven fabric models UniverFilter users can create weaves by either the conventional point paper technique or by using formulae. The conventional method is suitable for smaller weave repetitions, however if larger weave repetitions are required the formula method provides a more efficient mean by which to generate a weave. The woven fabrics used in this research work were configured in a balanced or square fabric form with an identical yarn linear density in Tex, number of ends and picks per cm. By standardising these fabric parameters the effect of different weaves can be systematically measured and identified. The three dimensional solid models of plain 1/1, twill 2/2 and 8-ends satin woven fabrics were generated in IGES format, Figure 5, which enables efficient transfer from UniverFilter to ABAQUS.

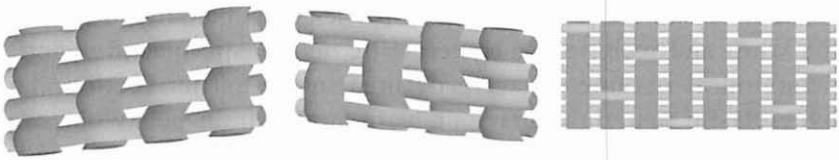

(a) (b) (c)

Figure 5: 3D Woven Fabrics Models (a) Plain 1/1 (b) 2/2 Twill (c) 8-ends Satin

Importing the Geometrical Models and Material Parameter Definition

The three dimensional geometry models of plain, twill and satin weaves were transported to the finite element analysis package, ABAQUS, for rendering and meshing, and combined with the warp and weft yarns, which were transferred separately from UniverFilter. This ensured that the transferred yarns are smooth surface interpolations able to accurately represent the woven fabric. This leads to excessive element face

generation and can lead to element convergence equilibrium problems, not only during meshing, but also when performing finite element computations, due to each face being seeded individually and generating increasingly smaller and more meshed elements. This problem was alleviated by combining all the yarn faces together into four faces; namely, face, back, top and bottom. Figure 6 presents an 8 ends satin warp yarn before and after face combination.

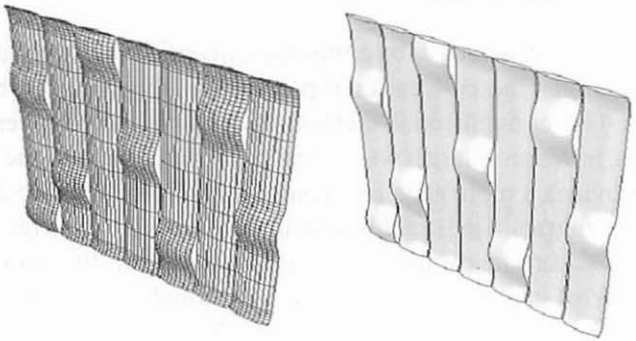

(a) (b)

Figure 6: Imported IGES Model (a) Before and (b) After Surface Combining

Once imported, the material properties must be defined for both the warp and weft yarns. Hyperelastic and elastic-plastic material behavioural parameters were defined in the earlier section. The hyperelastic material behaviour, yarn stress-strain behaviour, was scaled-down since the woven fabric models were 140 times smaller than the experimental samples and was necessary in order to ensure that the theoretical stress-strain results could be readily compared to the experimentally determined results. This was achieved with respect to a scaling factor derived based upon the initial fabric yarn length, the force applied in woven tensile strength test, the number of warp ends in the samples, the yarn cross sectional area, the warp crimp, the fabric length and the weave factor. The resultant equation, Equation 10, enables the stress experienced by the woven fabric under uniaxial tension, when a load is applied, to be incorporated into the model by dividing the number of ends by its respective yarn area. The equation also incorporates the number of yarn intersections, i, and floats, f, so that the yarn-stress scales with respect to the length of the float thereby reducing the yarn uniaxial tensile stress per increment with respect to the next

experimental load increment. The derived stress increment scale factor equation is presented below, Equation 10:

$$\sigma_{si} = \sum_{i=1}^{n} \frac{\sigma_i}{\frac{F_f}{A_y.E_w} \cdot \frac{(L_o + C_w)}{L_f} . W_f} \tag{10}$$

σ_{si} i = 1, 2, 3, ... , n number of increments
σ_i = yarn experimental stress at increment i
F_f = load applied to woven fabric during tensile
A_y = yarn area in woven fabric
E_w = warp ends
L_o = yarn length in fabric
C_w = warp crimp
L_f = fabric gauge length
W_f = $\frac{i}{f}$ weave factor; where i = number of intersections and
f = number of floats

Using Hooke's law, Equation 11, the plastic-elastic behavior of the woven fabric materials the experimentally determined stress-stress values were converted to stress and plastic strain values, thereby enabling evaluation beyond the yield point, with respect to Equations 11 and 12:.

$$\sigma_i = \sum_{j=1}^{6} C_{ij} \varepsilon_j \tag{11}$$

$$\varepsilon^{pl} = \varepsilon^{t} - \varepsilon^{el} = \varepsilon^{t} - \frac{\sigma}{E} \tag{12}$$

$$\sigma = \sigma_{norm} (1 + \varepsilon_{norm}) \tag{13}$$

where;

C = elastisicty tensor
ε = strain tensor
ε^{pl} = true plastic strain
ε^{t} = true total strain
ε^{el} = true elastic strain
σ = true stress

E = modulus
σ_{norm} = nominal stress
ε_{norm} = nominal strain

Contacts, Load, Boundary Conditions and Meshing

Surface-to-surface tie-constraints were implemented since this ensures that warp and weft surface interactions maintained at their points of contact throughout the simulated exposure to uniaxial loading. The warp surfaces were selected to act as the master surfaces since they were composed of fewer elements than the weft surfaces. Adopting this approach optimises the stress accuracy by minimizing the stress noise build-up in the elements at the points of contact between the surfaces, consequently yielding proficient stress distributions. The constraints applied are presented in Figure 7 below.

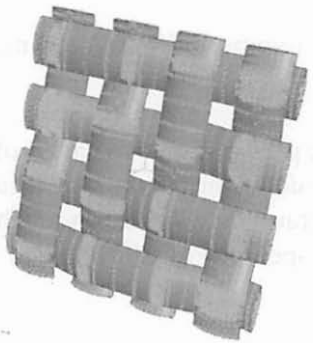

Figure 7: Surface Contact Constraints

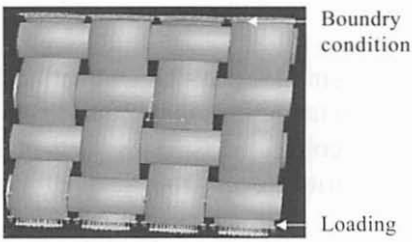

Figure 8: Load and "Encastre" Boundary Conditions

In order to enable simulation of the woven fabrics upon exposure to uniaxial tension the edges opposite the load are restrained by applying specific boundary conditions. The warp yarns were restricted to lengthwise and rotational movement, further to which "encastre" conditions were imposed whereby no rotational or translational movement at the origin of the yarns is permitted, Figure 8. The final preparatory phase prior to finite element analysis is meshing during which the woven fabric geometries are decomposed into smaller volumes composed of elements and nodes. Meshing is designed to simplify the solving of three dimensional problems involving partial differential equations by using linear matrix computations. Mesh generation is

achieved by seeding elements into a sequence of regular node intervals which breeds node positions and elements. The closer nodes are to each other the more and finer the elements. Fine meshes tend to yield more precise and accurate results, but at the expense of extensive computational times. The presented work uses a 4 linear node tetrahedral mesh element with 0.2 seeding, since woven fabrics have irregular geometries, especially with the crimps and floats presence, which the tetrahedral mesh elements can adapt to. A further assumption with respect to the application of a tetrahedral mesh is that strain displacement over the entire length of an element is constant. The application of this element type possesses three degree of freedom (d.o.f.) at the four nodes and a total of twelve d.o.f. per element [22]. The meshing procedure yields between 13,000 and 33,500 elements depending on the woven structures and the degree of crimp complexity. With respect to the element size the finite element analysis convergence requires between 30 and 75 minutes. Table 2 presents a summary of the number of elements for the warp and weft yarns investigated.

Table 2: Number of Elements

	Warp	Weft
Plain	20,553	23,248
Twill	13,332	13,311
Satin	30,025	33,287

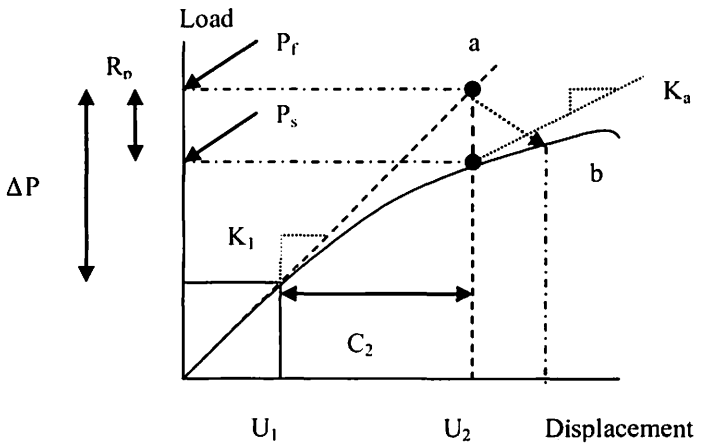

Figure 9: Equations Convergence Procedure

The magnitude of the uniaxially applied load to the woven fabrics with respect to the finite element method must attain computational equilibrium at each elemental increment, whereby the external, E, and internal, I, forces acting on the body must satisfy the following relationship:

$$E - I = 0 \tag{14}$$

Ensuring computational equilibrium at each incremental step is highly complex due to the inclusion of material properties, geometrical nonlinearities and surface contact issues. Iterative convergence, as presented in Figure 9, is required in order to compensate for the nonlinear behaviour of the individual elemental iterative solutions. For example, the structural internal force is recomputed with respect to the residual error, R_p, which is based on the displacement configuration, U_1, small load change, ΔP, and tangent stiffness, K_1. If R_p is zero, then the finite element computes the next load displacement iteration with respect to the load-displacement curve and the structure is accepted to be at equilibrium. If the R_p is not zero and within the stipulated tolerance limit of 0.5% of the average structural force, then the next displacement point is re-computed based on the previously acceptable displacement iteration. The structure's new equilibrium status is revised with respect to the last displacement correction, C_2, which must be relatively small compared to the total incremental displacement, $\Delta U_2 = U_2 - U_1$. If the displacement correction, C_2, is larger than 1% of last the displacement, ΔU_2, then a new iteration is performed. Otherwise, the structure is said to have achieved equilibrium for that iteration and simulation will progress to the next elemental increment. The incrementation is kept relatively small to enable efficient history dependent model effects to be evaluated; hence the load magnitude, Figure 8, must be adequate to ensure smooth incrementation, especially when handling non-linear implicit geometrical structural instabilities in the finite element analytical solutions.

Results and Discussion

Uniaxial tensile stress-strain

The hyperelastic model results for the plain weave 1/1 are compared with the corresponding experimental results and presented in Figure 10(a).

In general the theoretical and experiment results correlate well with each other, but the hyperelastic stress-strain curves have been separated into three zones, which correspond to deviation occurs between the stress-strain results. In Zone 1 (Strain 0-1.45%) the theoretical results exhibit higher stress than the experimental results. By comparison in Zone 2 (Strain 1.45-1.72%) the experimental and simulation results are almost identical. Beyond Strain 1.72% the experimental results exhibit greater stress than the model suggests and this constitutes Zone 3, which is indicative that the warp yarns are responding to uniaxial tensile loading. Similar results were observed for the woven twill and satin fabrics, Figures 11(a) and 12(a), respectively.

The stress-strain performance of woven plain fabrics is well-described by the elastic-plastic model, Figure 10(b), over a Strain % range twice that for the hyperelastic model. The model compares well with the experimental data up until Strain 2%, whereupon the experimental stress exceeds that predicted by the model until Strain 4%, which corresponds to plastic deformation at a stress of 37 MPa, where the model overpredicts the stress. Beyond a Stress of 4% the yarns begin to experience a reduced change in stress with strain percentage, which is a consequence of the extensional effect as the decrimping phase ends and the stress-strain behaviour at this juncture is governed by the extension of the deformed yarn. The twill and satin work presented in Figures 11(b) and 12(b), respectively, indicate large strain deformations of up to 6%. The elastic-plastic models for woven twill and satin fabrics compare well with the non-linear behaviour of

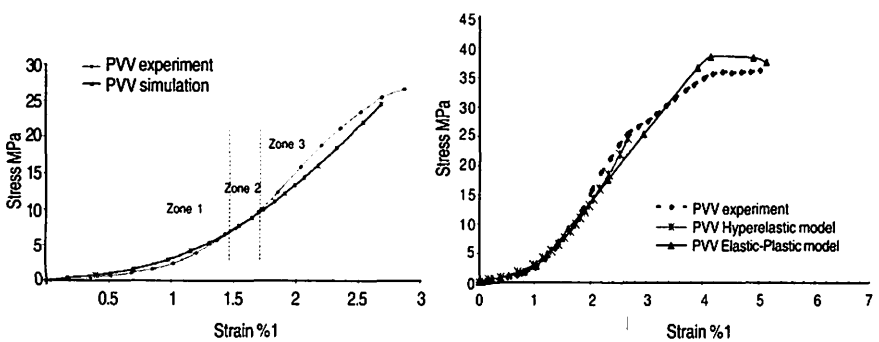

Figure 10: Comparative Stress-strain Plots with Respect to the (a) Hyperelastic and (b) Elastic-plastic Models for Woven Plain Fabrics

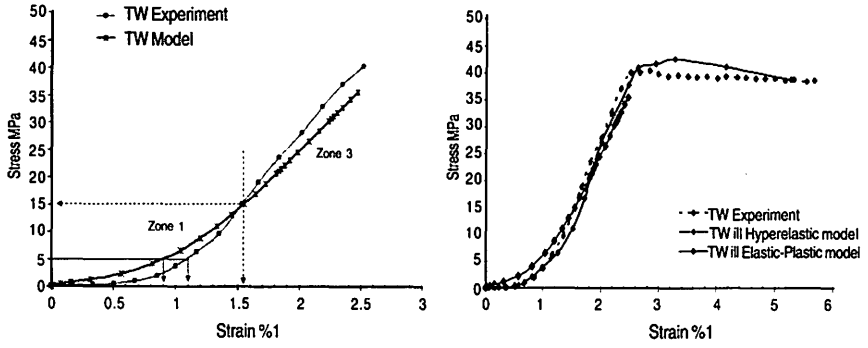

(a) (b)

Figure 11: Comparative Stress-strain Plots with Respect to the (a) Hyperelastic and (b) Elastic-plastic Models for Woven Twill Fabrics

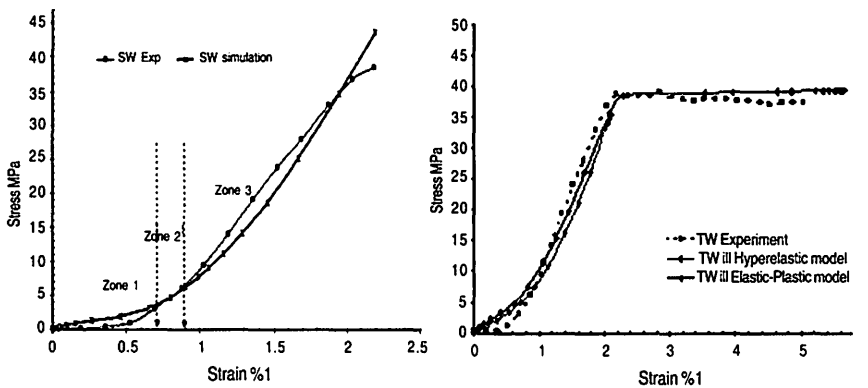

(a) (b)

Figure 12: Comparative Stress-strain Plots with Respect to the (a) Hyperelastic and (b) Elastic-plastic Models for Woven 8-ends Satin Fabrics

the experimental results up to and beyond the yield points. However the twill model overcalculates the stress experienced by the fabric at the yield point, but the satin model exhibits little or no overcalculation at the yield point. This may be attributed to longer floats used in satin weaves, hence the satin warp yarns respond faster to loading with minimal weft yarn interference during the unbending phase and eventual deformation.

The hyperelastic and elastic-model simulations of woven plain, 2/2 twill and 8-ends satin fabrics are summarised in Figures 13 (a) and (b). It

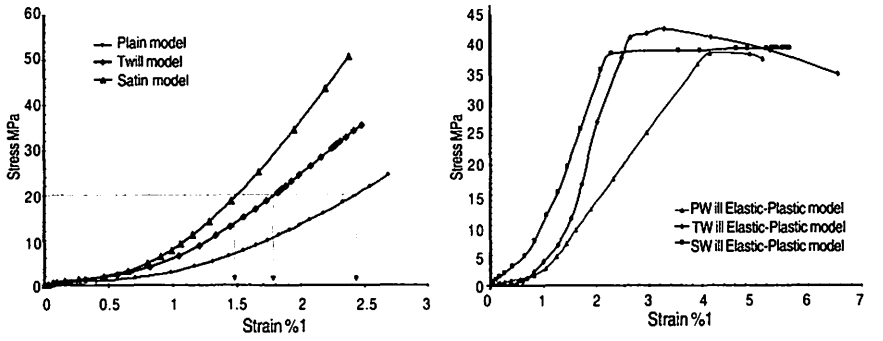

(a) (b)

Figure 13: Woven Plain, 2/2 Twill and 8-ends Satin Fabric Model Results

is evident that with respect to equivalent ends cm^{-1} and picks cm^{-1} the plain weave exhibits the lowest stress-strain compared to twill 2/2 and 8-ends satin. Furthermore the woven plain fabrics behave in the most nonlinear manner accompanied by a lower modulus of elasticity due to the presence of more crimps within their structure. Hence, the more extensive the yarn interfacings within a woven fabric structure, the higher the stresses created are in these regions, which culminates in lower overall stress-strain with higher strain percentages. For instance, at 20 MPa of stress the woven plain fabrics exhibit a strain percentage of 2.42%, whereas the satin and twill fabrics exhibit strain percentages of 1.47% and 1.87%, respectively. These results are consistent with those reported by Gasser *et al.* [7] for equal biaxial loading of plain, 2/2 twill and 3/2 twill, in which the woven structure with the longer float length, 3/1 twill, exhibits the highest loading capacity compared to the woven plain and 2/1 twill fabrics.

The hyperelastic and elastic-plastic models provide different perspectives of the modelling of woven fabrics undergoing uniaxial tensile strength testing, yet both are of equal value. For the hyperelastic model, the Ogden strain energy potential of the woven fabrics was determined with respect to the behaviour of long-chain molecules in elastomeric materials. The ABAQUS material module assumes that hyperelastic deformation is isotropic even though the materials consider exhibit anisotropy when undergoing stretching. The Ogden strain energy potential enables the inclusion of uniaxial yarn stress strain within the material property editor thus providing enhanced simulation accuracy. Although plain and satin hyperelastic models describe the experimental results well,

particularly in the low strain zone, they suffer from poor finite element convergence and are thus computationally ineffective. With this in mind, the elastic-plastic models were developed to improve the finite element convergence thus enabling larger strain results. This was achieved by defining the material to be elastic-isotropic and coupling this with computed plastic deformation data with a coarser elemental mesh. These models provide an interesting opportunity to study the strain distribution and compression stress within woven fabrics. The hyperelastic model was implemented to review the strain distribution effects during uniaxial loading, since it correlates well with experimental data at low strain percentages. In contrast, the elastic-plastic model was chosen to evaluate the compression forces exerted between the weft-warp node pairs, since it is capable of simulating larger strains. The following section describes the findings of this modelling work.

Strain Distribution in the FE Model

Strain in the woven fabrics has been evaluated further by comparing its distribution using finite element analysis models. The strain distributions and their respective levels determined using the FE model for woven plain 1/1, twill 2/2 and 8-ends satin fabrics are presented in Figure 14 and Table 3, respectively. Even though all the woven fabric models yielded positive strains in the warp direction, S_{22}, interesting strains were exhibited in the unloaded weft direction, S_{11}, and at the interlacing points. Most of the strains exhibited by the models in the warp direction are classified as Level 2 and 3 strain distributions. The positive strains in the warp yarns inherently influence strains in the weft yarns particularly at the crossover regions. Negative level 4 strains were found in the non-contact weft yarn regions, especially between two warp yarns; it is therefore possible to evaluate the effect of the level of crimp on the strain exhibited with woven plain, twill 2/2 and 8-ends satin fabrics. Less crimp interchange effects are exhibited in the satin warp yarns, because it yields strain results immediately upon loading, Figure 14 (c). The strain distribution presented in Figure 14 (c) exhibits Level 2 warp strains accompanied with Level 1 weft strains, which corresponds to the higher stress modulus for woven 8-ends satin fabrics than for woven plain and twill 2/2 fabrics, as presented in Figure 13.

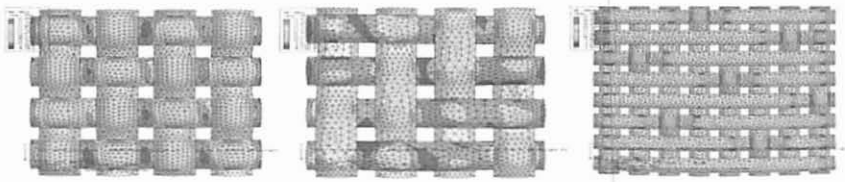

(a) (b) (c)

Figure 14: Strain Distributions from Finite Element Analysis of Woven (a) Plain (b) 2/2 Twill 2/2 (c) 8-ends Satin Fabrics

Table 3: Strain Distribution Levels

Level	Strain distribution classification
3	Positive strains, 1.3% to 2.68%
2	Positive strains, 0.5% to 1.3%
1	Positive strains, 0.07% to 0.5%
4	Negative strains 0 to 0.05%

Yarn Compression Effect

Compression analysis between warp and weft yarn node pairs was performed on neighbouring yarns using the elastic-plastic model. The compression force (MPa) was taken from the S_{33} material orientation with respect to its displacement (mm). The results for this analysis are presented in Figure 15. The plain weft yarn exhibits the highest compression stress (3.25 MPa) with displacement of 1.87×10^{-4} mm, Figure 15 (a). By comparison the satin weft compression exhibits the smallest stress (0.055 MPa) with a displacement of 0.22 mm, Figure 15 (c), which may be attributed to the compression force acting at the limited interlacing regions due to the use of longer floats. The consequence of which is inferior and linear warp compression stress-displacement upon uniaxial loading compared to tighter woven fabric structures, such as the plain woven fabric. Unlike the plain and satin woven fabrics in which either the weft or the warp yarns exhibit significantly different levels of stress with displacement, the twill woven fabric yarns exhibit comparable stress up to a displacement of 0.8 mm, Figure 15 (b). Ultimately the warp yarn exhibits a far greater stress and more so than any of the yarns considered in this analysis. It should be noted that the nodes in the finite element analysis are positioned at each of the corners

of the tetrahedral elements, which yields higher stress values compared than if the nodes were positioned closer to the core of the elements. The nodal compression pairs presented in Figure 15 (d) have enabled neighbouring nodal surface compression analysis to be performed.

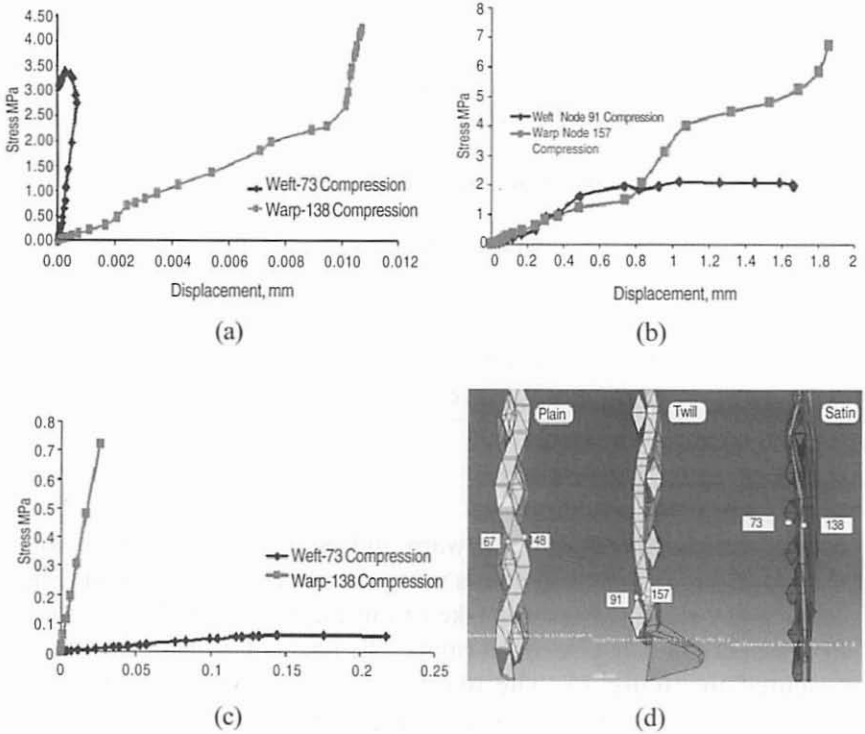

Figure 15: FE Compression Analysis of Warp and Weft Yarns for (a) Plain, (b) Twill, (c) Satin Woven Fabrics and (d) the Node Compression Pairs

Conclusion

Experimental and finite element analysis of plain 1/1, twill 2/2 and 8 ends satin woven fabrics has been performed using hyperelastic- and elastic-plastic-material models. The results indicate that 8-ends satin woven fabrics exhibit the highest stress-strain performance compared to plain and twill woven fabrics. The use of UniverFilter has enabled the accurate representations of woven fabrics for the purposes of simulation, thereby elucidating information regarding the stress

experienced by fabrics undergoing uniaxial loading with respect to surface to surface contact points.

The results of this work indicate that the stiff Zone 1 determined using the hyperelastic woven fabric models could be attributed to assuming that the yarns are monofilaments, rather than multifilament, as in real woven fabrics. It is also noted that the higher experimental woven fabric moduli for all woven fabrics in Zone 3 may be due to the capacity for yarns to move whilst under tension; whereas in the modelling it was assumed that the yarns are fused at a given position throughout the analysis. The elastic-plastic model describes experimentally determined results better than the hyperelastic model, especially in the case of plain and satin woven fabrics, furthermore it is able to achieve higher strain than the hyperelastic model in an acceptable computation time. Most importantly, this work suggests that it is possible to simulate compression forces in woven fabrics in a uniaxial manner unlike previous researchers who adopted a biaxial approach. Satin woven fabrics demonstrated the highest stress within the low displacement region, but twill woven fabrics indicate that the stress is distributed more equally between the weft and warp yarns up to a displacement of 0.8 mm.

Satin warp yarns respond immediately to loadings and yields a stronger fabric; plain and twill weave firstly have to decrimp upon loading, which culminates in higher stress at the interlacing regions and lead to a weaker fabric. Hence it can be concluded that the woven 8-ends satin fabrics better uniaxial loading performance is a consequence of the inherent lower crimp within the fabric, faster unbending rates and high yarn compression. The presented work enhances the present understanding and application of finite element analysis in the investigation of the mechanical properties of textile structures, specifically woven fabrics. Further work should be performed with respect to the modelling and finite element analysis of laminated aramid-based woven fabrics undergoing uniaxial loading.

References

[1] S.K. Mukhopadhyay and J. F. Partridge, 1999. *Automotive Textiles*. First ed.: The Textile Institute, 1-25.

[2] Horrocks and S. Anand, 2000. *Handbook of Technical Textiles, The Textile Institute*: Woodhead Publishing Limited, pp. 491-528.

[3] P. Boisse, 2005. Analysis of Mechanical Behaviour of Woven Fibrous Material Using Virtual Tests at the Unit Cell Level, *Journal of Materials Science*, 40, pp. 5955-5962.

[4] J.W.S. Hearle, and W.J. Shanahan, 1978. An Energy Method for Calculations in Fabric Mechanics, *Journal of Textile Institute*, 69(4), pp. 81-91.

[5] P.E. Lewis, and J.P. Ward, 1991. *The Finite Element Method. Principles and Application*, Addison-Wesley Publishing Company. pp. 416.

[6] M. Tarfaoui, and S. Akesbi, 2001. Numerical Study of the Mechanical Behaviour of Textile Structures, *International Journal of Clothing Science and Technology*, 13(3/4), pp. 166-176.

[7] M. Tarfaoui and S. Akesbi, 2001. A Finite Element Model of Mechanical Properties of Plain Weave. Colloids and Surfaces A: *Physicochemical and Engineering Aspects*, (187-188), pp. 439-448.

[8] C.G. Provitidis, and S.G. Vassiliadis, 2004. On the performance of the geometrical models of fabrics for use in computational mechanical analysis, *International Journal of Clothing Science and Technology*, 16(5), pp. 432-444.

[9] E.H. Glaessgen *et al.*, 1996. Geometrical and Finite Element Modelling of Textile Composites, *Composites Part B*, 27B(1), pp. 43-50.

[10] A. Gasser, P. Boisse and S. Hanklar, 2000. Mechanical Behavior of Dry Fabric Reinforcements. 3D Simulations versus Biaxial Test, *Computational Materials Science*, 17, pp. 7-20.

[11] P. Boisse, B. Zouari and A. Gasser, 2005. A Mesoscopic Approach for the Simulation of Woven Fibre Composite Forming, *Composites Science and Technology*, 65, pp. 429-436.

[12] Y. Duan, *et al.*, 2006. Finite Element Modeling of Transverse Impact on Ballistic Fabric, *International Journal of Mechanical Sciences*, 48, pp. 33-43.

[13] P. Potluri, and V.S. Thammandra, 2007. Influence of Unixial and Biaxial Tension on Meso-Scale Geometry and Strain Fields in a Woven Composite, *Composite Structures*, 77, pp. 405-418.

[14] P. Boisse, *et al.*, 2001. Meso/macro-Mechanical Behaviour of Textile Reinforcements for Thin Composites, *Composites Science and Technology*, 61, pp. 395-401.

[15] *Abaqus CAE Vol 2: Analysis*, Simulia.

[16] G.A.V. Leaf, 2002. Analytical Woven Fabric Mechanics, *International Journal of Clothing Science and Technology*, 14(3/4), pp. 223-229.

[17] G.A.V. Leaf, 2004. The Mechanics of Plain Woven Fabric, *International Journal of Clothing Science and Technology*, 16(1/2), pp. 97-107.

[18] Y. Duan, *et al.*, 2005. Modeling the Role of Friction During Ballistic Impact of High-Strength Plain-Weave Fabric, *Composite Structures*, 68, pp. 331-337.

[19] M. Valizadeh, *et al.*, 2009. Finite Element Simulation of Yarn Pullout Test for Plain Woven Fabrics, *Textile Research Journal*, pp. 1-12.

[20] F.T. Pierce, 1937. The geometry of cloth structure, *Journal of Textile Institute*, 28, pp. 45-96.

[21] X. Ai, 2003. *Geometric Modelling of Woven and Knitted Fabric for Technical Application*, Department of Textiles. University of Manchester: Manchester.

[22] R.D. Cook, 1995. *Finite Element Modeling for Stress Analysis*: John Riley & Sons, Inc.